ACS OMEGA

http://pubs.acs.org/journal/acsodf

Article

Water Droplets Tailored as Wax Crystal Carriers to Mitigate Wax Deposition of Emulsion

Qianli Ma,* Chuanshuo Wang, Yingda Lu, Yang Liu, Xiaofang Lv, Shidong Zhou, and Jing Gong

Cite This: *ACS Omega* 2023, 8, 7546−7554

Read Online

ACCESS | Metrics & More | Article Recommendations | Supporting Information

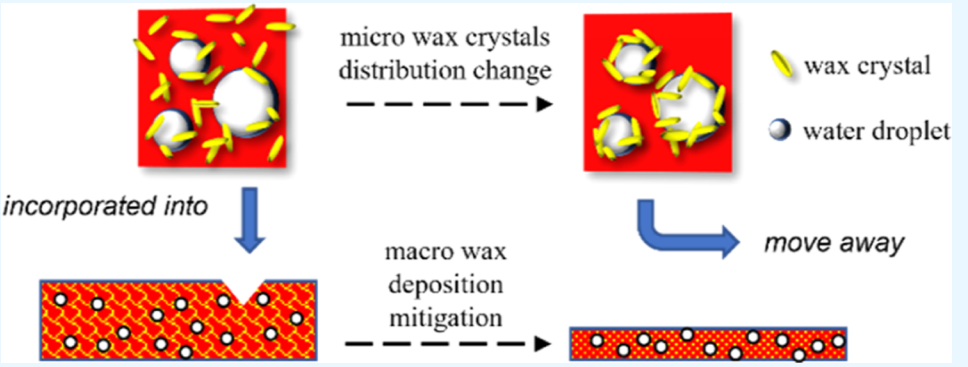

ABSTRACT: This study explores how the micro-distribution change of wax crystals from the continuous oil phase to the oil−water interface mitigates the macro wax deposition of an emulsion. Two types of interfacial actions between wax crystals and water droplets, interfacial adsorption and interfacial crystallization, which were induced by two different emulsifiers, sorbitan monooleate (Span 80) and sorbitan monostearate (Span 60), respectively, were detected by differential scanning calorimetry and microscopy observation. The wax interfacial crystallization promoted by Span 60 resulted in the wax being nucleated directly at the oil−water interface prior to the continuous oil phase, conferring the nascent wax crystals and water droplets to be combined as coupled particles. The utilization of the wax interfacial crystallization behavior to hinder wax deposition of an emulsion was further explored. When the coupled wax crystal−water droplet particles were formed during the wax deposition process, water droplets acted as wax crystal carriers, entraining these nascent wax crystals to disperse in the emulsion, which significantly reduced the amount of wax crystals available to form the network of the deposit. In addition, this change also led to the basic structural units in the wax deposit evolving from wax crystal clusters/networks to water droplet flocs. The study elucidates that through adjusting the dispersion of wax crystals from the oil phase to the oil−water interface, water droplets could act as a functional component to tailor the properties of the emulsion or resolve related flow and deposition problems in pipeline transportation.

1. INTRODUCTION

The rational utilization of water droplets in oil continuous emulsions has received much attention due to its ability to tailor the properties of emulsions required by products. Dispersed water droplets commonly act as fillers in these functional emulsified products, which have been explored in various studies.[1−4] For example, one low-fat spread was developed by emulsifying water into a cocoa butter matrix.[5] Reduced saturated fats and the caloric load in these water-filling alternatives make them healthier than traditional spreads. Moreover, the addition of water in the form of a water-in-oil emulsion created a softer texture for lipstick, one typical wax-based cosmetic product, and improved its moisturizing properties.[6] One key issue of these water-in-oil emulsions is maintaining their stability during the long-term static storage.[7] This stability depends greatly on the interaction between water droplet fillers and fat/wax crystals dispersed in the continuous oil phase.[8] These crystals either aggregate as a spatial network that physically encloses the water droplets, thereby preventing droplet collisions,[9,10] and/or are modified by an emulsifier as an interfacial attaching species to create a solid shell around individual water droplets, thereby hindering the contact, flocculation, and coalescence of droplets.[11−15] The stability of the emulsion is maintained by these two mechanisms.[16] Moreover, there are two kinds of interfacial attachment. Moreover, there are two kinds of interfacial attachment. One indicates that the interfacial crystallization of fat/wax molecules was mediated by the chosen emulsi-

Received: October 22, 2022
Accepted: February 6, 2023
Published: February 15, 2023

ACS Publications

© 2023 The Authors. Published by American Chemical Society

https://doi.org/10.1021/acsomega.2c06809
ACS Omega 2023, 8, 7546−7554

fier,[7,17−22] while another denoted that the fat/wax molecules first crystallized in the bulk and the emulsifier then promoted these crystals to be adsorbed at the oil−water interface.[23−25] The composition and interaction of the emulsifier and fat/wax crystals may dictate the specific interfacial attachment methods of particles to water droplets, where Ghosh et al.[16] found that the heterogeneous crystallization of a fat, hydrogenated canola oil, was promoted by one emulsifier, glycerol monostearate, but the interfacial adsorption of fat crystals changed when the emulsifier was changed to glycerol monooleate.

Based on the above investigations, it is noticed that water droplets not only act as fillers to tune the qualities of the matrix and create functional products but also change the distribution of crystals, which aggregate a number of crystals from the continuous oil phase to the oil−water interface, either by interfacial crystallization, which was explored by Ueno et al.[19] as the interfacial heterogeneous nucleation that accelerated by the freezing of a high-melting point emulsifier permitted the wax to crystallize at the oil−water interface prior to the oil phase, or interfacial adsorption, referring to the adsorption of fat crystals around water droplets that permitted droplets to tune the structure of the crystal network in the emulsion, which was used to produce the desired rheological properties of the emulsion explored by Rafanan and Rousseau.[2] The change in wax crystal distribution caused by the presence of water droplets inspired us to conduct the present study. Even though water filler applications have been used in the food and cosmetics industries, little is known regarding how to achieve a positive effect from the presence of water droplets in crude oil. As the water flooding technology is widely used to enhance oil recovery in the petroleum industry,[26] a water-in-waxy crude oil emulsion is usually formed during pipeline transportation.[27] When the emulsion flows through a pipe in a cold area, as the temperature is lower than the critical temperature, the temperature where the wax molecules dissolved in the oil phase begin to nucleate and crystallize, wax deposition occurs, in which wax crystals form and aggregate into a deposit on the pipe wall. Also, the critical temperature is usually regarded as the wax appearance temperature (WAT) in this field.[27,28] The formation of the wax deposit gel, as shown in Figure 1, causes a serious blockage in the pipe flow section, reducing the production and thereby posing a great challenge for flow assurance.[29] Traditional methods to remove the deposit include a thermal treatment to melt the formed wax crystals, chemical additives to slow down wax crystal aggregation, and mechanical scraping to remove the formed deposit layer.

Figure 1. Exhibition of the wax deposit formed in a pipe.

However, these methods are far from optimal in some conditions, where thermal treatment consuming extra heat energy is costly[30] and scraping cannot meet the requirements of continuous production.[31] Moreover, additives are expensive and not universal, indicating that they are not suitable for all wax deposition problems.[32] Therefore, an alternative approach considering the functional role of water droplets in the wax deposition process is necessary.

Since the water filler concept is used to design functional products in the food and cosmetics industries, in the petroleum industry, a similar concept that water serves as wax crystal carriers for pipe flow transportation is now considered. The objective of the present study was to demonstrate how the presence of water droplets in waxy oil emulsions significantly mitigates the wax deposition process. Two emulsifiers were employed with two different types of interfacial attachments: sorbitan monooleate (Span 80) promoted the interfacial adsorption of wax crystals,[11] whereas sorbitan monostearate (Span 60) with stearic acid as the hydrophobic moiety directly facilitated the crystallization of wax molecules at the oil−water interface.[33] The nascent tiny wax crystals induced by the latter emulsifier naturally attached with water droplets and were then entrained by water droplets to disperse in the emulsion rather than be deposited on the cold pipe wall. Therefore, the formation of the wax deposit was hindered. Such an approach offers the opportunity to adjust the aggregation of dispersed particles/crystals and droplets in an emulsion, where the desired structure is needed to optimize the multiphase flow in pipeline transportation containing wax crystals, gas hydrates, or sand particles.

2. MATERIAL AND METHODS

2.1. Materials. A kind of mineral oil, LP15, with the kinematic viscosity of 16.0 $mm^2 \cdot s^{-1}$ and the density of 0.856 $g \cdot cm^{-3}$ at 37.8 °C, purchased from Yan Shan Petrochemical Company, was employed as the oil phase. Highly refined 58# paraffin, obtained from Daqing Petrochemical Company, was used as wax. Deionized water with a resistivity of >15 MΩ·cm was employed as the aqueous phase. Two oil-soluble surfactants composed by the same hydrophilic moiety with a purity of > 99%, Span 80 (sorbitan monooleate) with an oleic chain as the hydrophobic moiety and Span 60 (sorbitan monostearate) with a stearic chain as the hydrophobic moiety, were used as emulsifiers. All chemicals were utilized without any further treatment.

2.2. Emulsion Preparation. Three kinds of waxy oils that were identified by the three different surfactant compositions, 0.5 wt % Span 80, 0.25 wt % Span 80 + 0.25 wt % Span 60, and 0.5 wt % Span 60, were prepared. Based on the mass of the oil phase, 5.0 wt % paraffin wax and 0.5 wt % surfactant were mixed into the mineral oil. All materials were then heated to 65.0 °C for 2 h to ensure that all substances were fully dissolved in the mineral oil. After that, waxy oils were obtained.

For emulsion preparation, waxy oil was gradually cooled down to 35.0 °C and maintained at this temperature for 30 min. Then, based on the volume of waxy oil, water that was also heated to 35.0 °C was gently poured into the oil phase with a volume ratio 20.0 vol %. A stirring speed of 500 rpm was applied by an IKA stirrer (Eurostar 20 digital, IKA, Germany) for 15 min to emulsify oil and water phases. Afterward, three waxy oil emulsions were obtained, which were also marked by the surfactant compositions as 0.5 wt % Span 80-doped emulsion, 0.25 wt % Span 80 + 0.25 wt % Span 60-doped

https://doi.org/10.1021/acsomega.2c06809
ACS Omega 2023, 8, 7546−7554

emulsion, and 0.5 wt % Span 60-doped emulsion. The drop test method was used to identify the type of emulsion. The drop of each emulsion was dispersed in the mineral oil but remained as drops on the surface of water, indicating that all emulsions were water-in-oil emulsions.

2.3. Thermal Analysis. A thermal analysis device, a differential scanning calorimeter (Q2000, TA Instruments, USA), was used to measure the WAT of waxy oil as well as emulsion samples. In addition, the content of precipitated wax in the deposit was also determined by the thermal analysis.

The thermal test was conducted as a small quantity of samples (approx. 4−8 mg) were collected into aluminum crucibles and sealed by lids. Then, the crucible was taken to the device, waiting for heating and cooling processes. The sample was first heated to 60.0 °C and kept at this temperature for 10 min. Then, it was cooled down to −20.0 °C with a cooling rate of 5.0 °C·min^{-1}. Following each test, a thermogram plotting the heat flow versus temperature was obtained. The temperature when the heat flow deviated from the baseline was determined as the WAT point of the sample, and the precipitated wax content was calculated by integrating the area between the baseline and the heat flow curve.

2.4. Microscopy Observation. A polarized light microscope (BX51, OLYMPUS, Japan) was used to characterize the morphology of the emulsion and deposit as its loading platform was equipped with a thermally controlled plate (80.0 to 0.0 °C with a precision of ±0.1 °C). A micro digital image analysis system (any micro DSS, 10 MEGA Digital Shoot System, China) was employed to obtain the microstructure of the sample. The images were subsequently analyzed by the software ImageJ 1.47V (National Institute of Mental Health, Rockville, USA).

The specific observation procedure was as follows: a trace of the test sample was placed on the viewing slide at the set temperature of 35.0 °C for the emulsion and at room temperature, 21−23 °C, for the deposit. For the emulsion sample, the temperature, 35.0 °C, was higher than the WAT of the sample, indicating that no wax crystallized out to influence the size measurement of water droplets in the emulsion. Then, the emulsion was cooled down with a cooling rate, 5.0 °C·min^{-1}. When the temperature was decreased to WAT of each emulsion, the nascent wax crystals were clearly recorded to show the initial interaction between wax crystals and water droplets. For the wax deposit sample, the morphology of the deposit was clearly photographed at room temperature, showing the basic structures that were organized in the deposit.

2.5. Wax Deposition Apparatus. The cold finger apparatus was employed to carry out the wax deposition experiment, which was widely used in the previous study.[27,35,37] The schematic diagram of the cold finger is illustrated in Figure 2. There were two temperatures, T_1 and T_2, maintained by two water baths. T_1 was equal to the temperature of the emulsion flowed in the pipe, whereas T_2 was equal to the temperature of the pipe wall affected by the external environment. T_1 was higher than T_2, suggesting that heat was lost from the pipeline to the surroundings during the oil transportation process, and, T_2 was set to equal or lower than the WAT, allowing the wax to crystallize out and deposit on the pipe wall as shown in Figure 1.

The temperature of the cold rod, T_2, was kept at 15.0 °C, while the temperature of the reservoir, T_1, was set at 35.0 °C. Therefore, the temperature difference T_1 > WAT > T_2 was established, which determined the radial temperature gradient

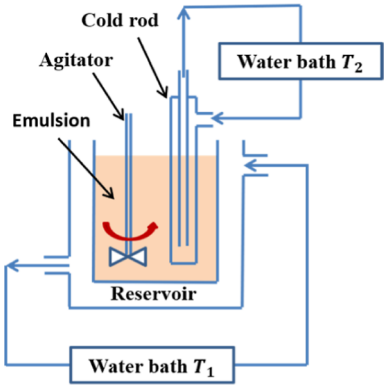

Figure 2. Schematic diagram of the cold finger apparatus.

from the fluid to the pipe wall. In addition, a stirring speed of 350 rpm was applied by the agitator for the stirring condition, simulating the pipe flow shearing effect on the wax deposit. Once the cold rod was immersed in the emulsion, the wax deposition experiment began as the deposit formed and grew on the cold rod. The deposition process lasted until the mass/thickness of the deposit remained consistent, and in this experiment, the constant deposit mass finally appeared after 12 h of deposition time. The deposit was then sampled to measure the water and wax content in the deposit. The wax deposition experiment for each emulsion sample was repeated in triplicate.

2.6. Water Content in the Deposit. A Karl Fischer moisture analyzer (T635, SDXW analysis, China) with a test range from 5 μg to 30 mg and a sensitivity of 0.1 μg was utilized to examine the amount of water in the deposit. The wax deposit was carefully scraped off from the cold rod, weighed on the scales, and then mixed with an equal weight of mineral oil. The mixture was then dropped into the Karl Fischer reagent, and the weight of water was precisely measured. The water content in the deposit was then calculated.

3. RESULTS AND DISCUSSION

3.1. Distribution of Water Droplets. The diameter distribution of water droplets for the three emulsifier-doped emulsions at 35.0 °C is shown in Figure 3. The percentages of droplets for the three emulsions in each diameter range were comparable with little variation, indicating that two similar surfactants, Span 80 and Span 60 used separately or jointly, yielded analogous emulsification results when the dosage of the surfactant in three emulsions was identical, 0.5 wt %. The dispersion of water droplets, such as the average droplet diameter and the narrow or broad size distribution, could impact the wax deposition process of the emulsion,[34] leading to a decreased deposit thickness[35,36] or a soft deposit layer.[37] Therefore, the similar diameter distribution of water droplets ruled out the possibility that the following wax deposition mitigation was caused by the size variation of water droplets in different emulsifier-doped emulsions.

3.2. Wax Crystallization Temperature in Emulsions. The heat flow curves of three emulsions and waxy oil are displayed in Figure 4. When compared to the WAT of waxy oil, 28.2 °C, marked on the black curve, the WAT of Span 60-based emulsions was certainly increased with a value of 31.4 °C for the 0.5 wt % Span 60 emulsion and 30.0 °C for the 0.25 wt % Span 80 + 0.25 wt % Span 60 emulsion. However, the WAT

https://doi.org/10.1021/acsomega.2c06809
ACS Omega 2023, 8, 7546−7554

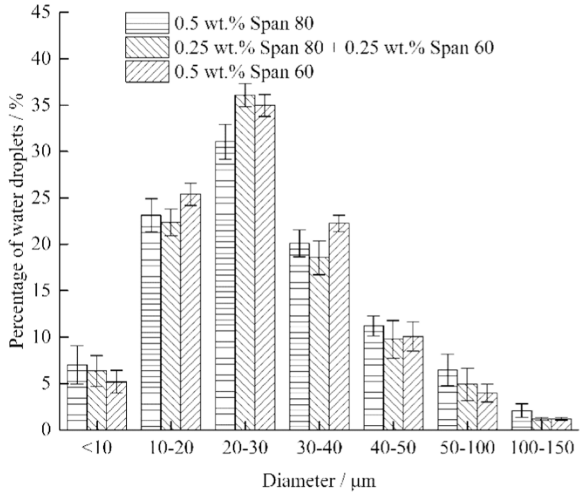

Figure 3. Distribution of water droplets for three emulsions prepared by different surfactant compositions at 35.0 °C.

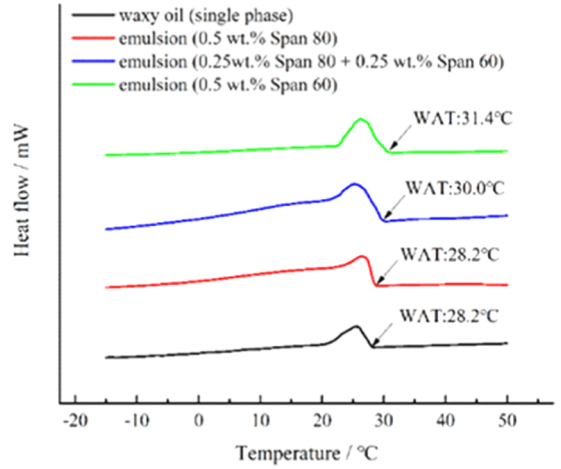

Figure 4. Heat flow curves of waxy oil and emulsions prepared by different surfactant compositions with WAT marked in each curve.

of the emulsion prepared by 0.5 wt % Span 80 was consistent with that of the waxy oil at 28.2 °C. From the different WATs shown in this image, it was noted that the wax crystallization temperature in the emulsion was certainly affected by Span 60. The more Span 60 contained in emulsion, the higher the WAT of the emulsion is.

More details provided by the morphology observation of the emulsion in Figure 5 were used to explain the increase of WAT for Span 60-containing emulsions. The initial wax crystallization sites for Span 60-doped emulsions were the oil−water interface, in contrast with the oil phase for Span 80-doped emulsions, suggesting that Span 60 facilitated the interfacial nucleation and crystallization of wax. Such interfacial heterogeneous nucleation characterized by the increase of WAT has been widely explored and elucidated from the opinion of the surfactant−wax molecular complementarity.[7,16−19] The wax interfacial crystallization induced by Span 60 may be resulted from the better structural matching between the hydrophobic moiety of Span 60 and the long chain alkanes in paraffin wax. The hydrophobic moiety of Span 60 was the stearic acid chain, which may facilitate the crystallization of the saturated alkane chains of wax at the oil−water interface compared with the unsaturated oleic acid chain

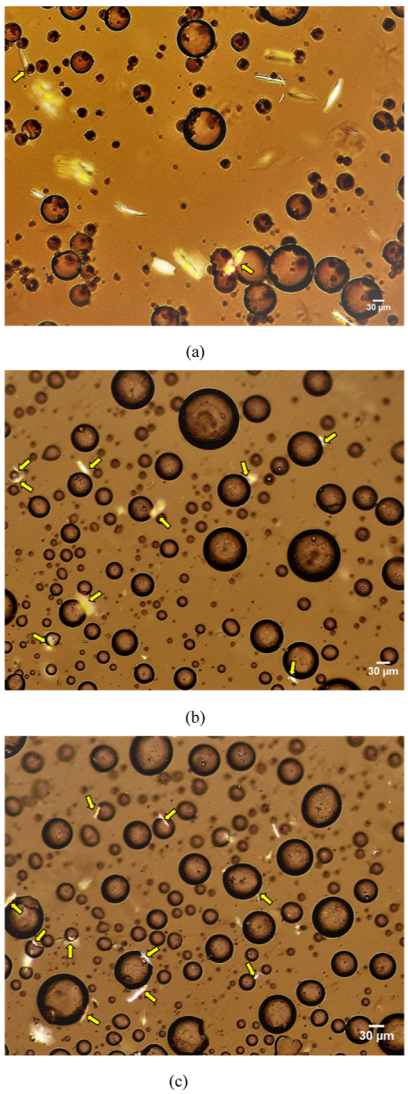

Figure 5. Morphology of emulsions with temperature cooled down to their corresponding WATs, where yellow arrows mark the wax crystals attached around the water droplets through interfacial adsorption in image (a) and interfacial crystallization in image (b,c). Samples: (a) 0.5 wt % Span 80-based emulsion at WAT, 28.2 °C; (b) 0.25 wt % Span 80 + 0.25 wt % Span 60-based emulsion at WAT, 30.0 °C; and (c) 0.5 wt % Span 60-based emulsion at WAT, 31.4 °C.

of Span 80. The promoted wax crystallization by surfactant Span 60 in emulsion was determined.

3.3. Morphology of Emulsions at WATs. The comparison of the distribution position of nascent wax crystals in the three emulsions at their tested WATs is shown in Figure 5. The distribution position of wax crystals for three emulsions with a statistically significant difference is summarized in Supporting Information S1. For the 0.5 wt % Span 80-based emulsion at the corresponding WAT, 28.2 °C, as shown in Figure 5a, wax crystals were mostly dispersed in the bulk oil phase, while few crystals marked by the yellow arrows are located around water droplets. As the WAT of this emulsion was equal to that of waxy oil, the interfacial action resulted in wax crystals attached with water droplets, regarded as interfacial adsorption, which was induced by the synergistic effect between surfactant Span 80 and wax crystals.[11]

In contrast to Figure 5a, images in Figure 5b,c report the wax crystallization behavior of emulsions formulated by Span

https://doi.org/10.1021/acsomega.2c06809
ACS Omega 2023, 8, 7546−7554

60 at their WATs. Wax crystals marked by the arrows in both images illustrated that the original wax crystallization site was the oil−water interface, not the continuous oil phase like that of the 0.5 wt % Span 80 emulsion. The interfacial action of wax transformed from adsorption by Span 80 to crystallization by Span 60, where interfacial heterogeneous crystallization permitted a higher liquid−solid phase transition temperature that has been examined in Figure 4. Therefore, the change of the wax crystal distribution position was achieved by altering the interfacial action from adsorption with Span 80 to crystallization with Span 60. The conversion further reduced the possibility that wax crystals aggregated with each other in the continuous oil phase and promoted the formation of coupled wax crystal−water droplet particles.

3.4. Wax Deposit Thickness of Emulsions. The micro-transfer of wax crystals from the continuous oil phase to oil−water interface is examined in the above section and now is utilized to investigate its effect on wax deposition mitigation.

The wax deposit thicknesses for three emulsions are shown in Figure 6. Sample numbers 1, 2, and 3 represented the

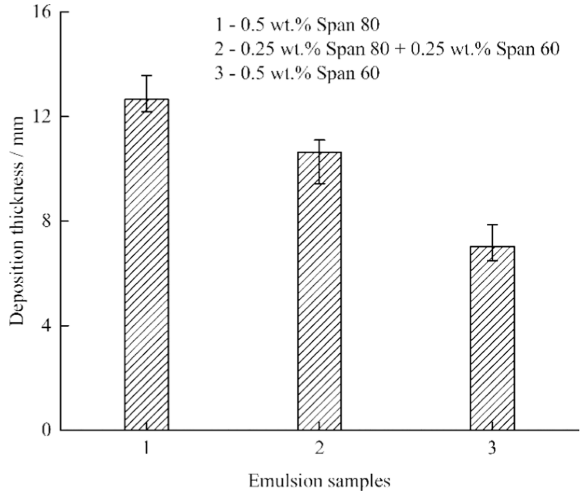

Figure 6. Wax deposit thickness of emulsion samples prepared by different surfactant compositions.

emulsions formulated by 0.5 wt % Span 80, 0.25 wt % Span 80 + 0.25 wt % Span 60, and 0.5 wt % Span 60, respectively. As can be seen from Figure 6, the thickness decreased with the increase usage of Span 60 in the emulsion, with specific thicknesses of 12.7, 10.6, and 7.0 mm in order of samples. The correlation was detected as the surfactant Span 60 provided the possibility to reduce the wax deposit. Experimental conditions that affected the wax deposition process such as the temperature gradient (35.0−15.0 °C), wax concentration (5.0 wt %), agitation intensity (350 rpm), water content of the emulsion (20.0 vol %), and size distribution of water droplets, which are shown in Figure 3, were kept consistent. Therefore, the mitigation result was not attributed to these parameters and was analyzed from the different interfacial actions of wax crystals induced by the two surfactants, Span 80 and Span 60. Further investigation of the thickness decrease was accompanied with the effect of interfacial action on the component and structure of the wax deposit.

Wax crystals and water droplets were the two main components to form the structure of the wax deposit with entrapped liquid oil phase. Wax crystals aggregated into clusters and spanned the network of the deposit, while some water droplets,, were integrated into the wax crystal network through wax interfacial adsorption.[27] Thereby, in order to explore which component resulted in the decrease of deposit thickness, the water and wax content in the deposit were determined. Moreover, the morphology of the three wax deposits was observed to illustrate the evolution of structures in the deposit.

3.5. Water and Wax Content in the Deposit. The water content in the wax deposit was tested by the moisture analyzer, and the results are shown in Figure 7a, reporting a similar

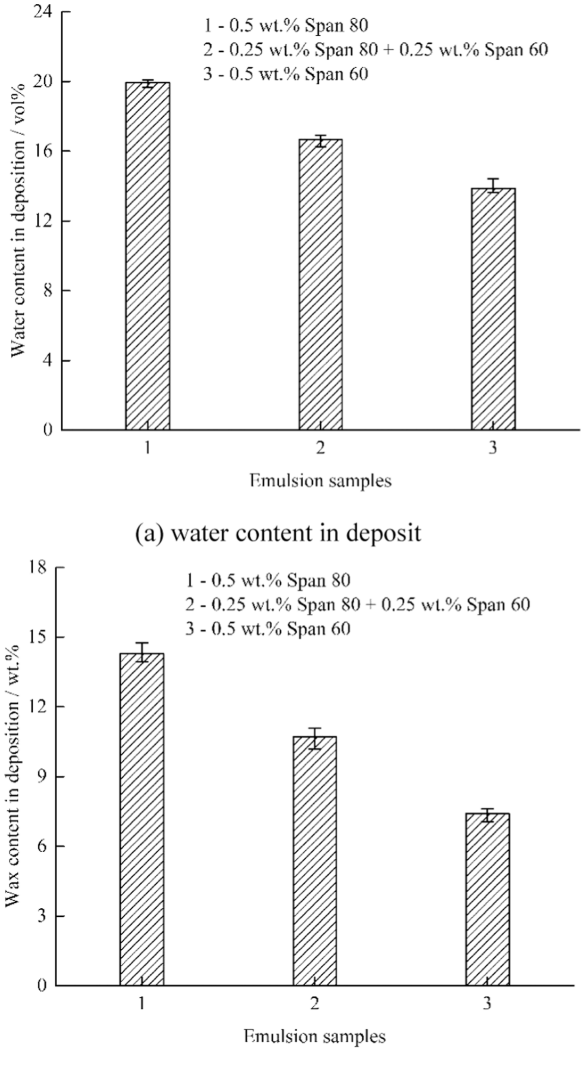

Figure 7. Water and wax content in the wax deposit for emulsion samples prepared by different surfactant compositions.

decrease trend to that of thickness in Figure 6. The more the Span 60 that is used in the emulsion, the less the water that exists in the corresponding deposit. The water content in the deposit for sample 1 was 19.9 vol %, which was almost equal to the water content in the emulsion, indicating that water droplets were simultaneously involved in the formation of the wax deposit. However, in the case of samples 2 and 3, with the increase in the dosage of Span 60 used in the emulsion, water droplets were less likely to be trapped in the deposit, with content of 16.7 and 13.9 vol %, respectively.

https://doi.org/10.1021/acsomega.2c06809
ACS Omega 2023, 8, 7546−7554

The wax content in the deposit for the three samples suggested the analogous tendency of the thickness and water content of the wax deposit, reported to be 14.3, 10.7, and 7.4 wt % in the order of the sample, as shown in Figure 7b. As the wax crystals were the basic components to form the volume-spanning network of the deposit, the less wax content presented in the deposit suggested that the dimension of the network in the deposit was restricted, giving rise to a reduced deposit thickness.

Regarding the water and wax content change in the deposit of the three emulsions, the wax deposition mitigation process for Span 60-doped emulsions was supposed to be as follows: due to the crystallization site being transferred from the continuous oil phase to the oil−water interface for the emulsion prepared by surfactant Span 60, the nascent wax crystals originally resided at the surfaces of the droplets, resulting in the coupled wax crystal−water droplet particles like those shown in Figure 5b,c. As no wax crystals formed in the continuous oil phase to aggregate into the network, which further constrained the movement of water droplets, these water droplets in Span 60-doped emulsions acted as wax crystal carriers, conferring wax crystals to disperse in the emulsion rather than deposit on the cold rod. Ultimately, the fundamental components in the deposit, water droplets, and wax crystals were consequently decreased, which is in line with the test results of a thinner thickness in Figure 6 as well as the lower wax and water content in Figure 7.

3.6. Morphology of the Wax Deposit. In order to verify the effect of interfacial action on the morphology of the deposit, the interplay between wax crystals and water droplets in the deposit was observed. The two components in the wax deposit, wax crystals and water droplets, generated three types of interaction: (1) a water droplet and a water droplet comprised water droplet flocs; (2) a wax crystal and a wax crystal aggregated as wax crystal clusters; and (3) a wax crystal and a water droplet coupled together as wax crystal−water droplet agglomerations. These three structural units basically set up the structure of the wax deposit. The proportion of each unit in the deposit is discussed to comprehend the wax deposition mitigation process.

For the 0.5 wt % Span 80-based emulsion, cases of structural units are marked in Figure 8a. Structural unit (3) wax crystal−water droplet agglomerations and structural unit (2) wax crystal clusters marked in this image consisted of the main structure in the deposit with few scattered water droplet flocs as unit (1). The interfacial adsorption of wax crystals induced by Span 80 marked by yellow arrows facilitated the combination of crystals with water droplets, which finally developed into structural unit (3). The specific process described that wax molecules were first crystallized in the continuous oil phase and then aggregated into a network and/or adsorbed onto surfaces of water droplets through movement and collision,[38] forming structural unit (2) wax crystal clusters and/or structural unit (3) wax crystal−water droplet agglomerations. These two units precipitated on the cold rod and gradually organized the wax deposit.

When a half dosage of Span 80 was replaced by Span 60 to prepare emulsion, the corresponding wax deposit exhibited a different microstructure, as shown in Figure 8b. Fewer wax crystal−water droplet agglomerations, unit (3), were presented in this case in contrast with that in Figure 8a. Instead, two structural units, unit (2) wax crystal clusters and unit (1) water droplet flocs, that were formed by the same species of particles

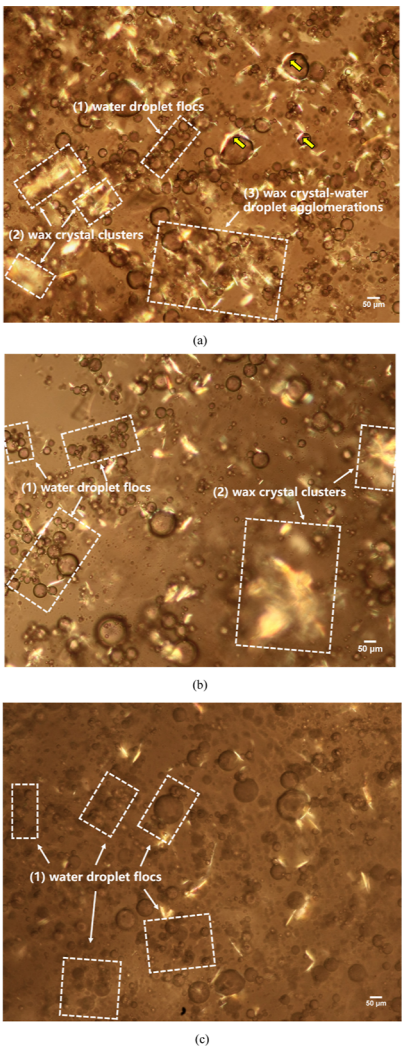

Figure 8. Polarized microscopy images of the thin film of the wax deposit for three emulsion samples prepared by different surfactant compositions with specific structural units: (1) water droplet flocs, (2) wax crystal clusters, and (3) wax crystal−water droplet agglomerations marked in each image. Samples: (a) 0.5 wt % Span 80-doped emulsion with three yellow arrows marking the interfacial adsorption of wax crystals; (b) 0.25 wt % Span 80 + 0.25 wt % Span 60-doped emulsion; and (c) 0.5 wt % Span 60-doped emulsion.

constituted the deposit. This change indicated that the interfacial crystallization caused by Span 60 affected the finial morphology of the deposit to a certain extent, retarding the formation of two different particles' agglomerations. According to the observation of the three structural units in Figure 8a, the size of agglomeration was large than that of the wax crystal clusters as well as the water droplet flocs, and the lack of agglomerations may be responsible for the decrease of the deposit.

The third morphology of deposit for the 0.5 wt % Span 60-doped emulsion is exhibited in Figure 8c. The fewest wax crystals were presented in this deposit compared with that in Figure 8a,b. Structural unit (1) water droplet flocs occupied the major space of the deposit, while wax crystal clusters and two particles' agglomerations were hardly observed in this case. The evolution of structural units in the three deposits demonstrated that the amount of wax crystals was gradually reduced with the increase of Span 60 used in the emulsion.

https://doi.org/10.1021/acsomega.2c06809
ACS Omega 2023, 8, 7546−7554

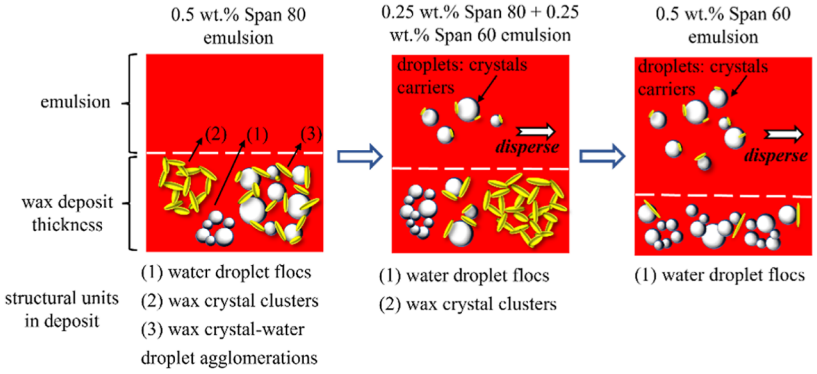

Figure 9. Schematic diagram of the water droplets tailored as wax crystals carriers by Span 60 with the transformation of structural units depicted in each deposit. Yellow flakes represent wax crystals; white spheres represent water droplets; dark blue circles around water droplets represent those adsorbed by the surfactant; and the red background represents the continuous liquid oil phase.

Combined with the interfacial crystallization triggered by Span 60, it was regarded that during the wax deposition process, the nascent wax crystals were originally formed at the oil−water interface and then entrained by these water droplets. Water droplets changed as wax crystals carriers, promoting wax crystals to disperse together with water droplets in the emulsion under the stirring condition of the system rather than allowing crystals to aggregate into clusters, and formed the basic networks of the deposit. Therefore, the micro-distribution change of wax crystals from the continuous oil phase for Span 80 to the oil−water interface for Span 60 led to the macro wax deposition mitigation. Due to the sharp temperature gradient from 35.0 to 15.0 °C, wax was rapidly crystallized in the initial deposition period, and several crystals were not entrained away with water droplets into the emulsion but were left in the deposit, which is observed in Figure 8c.

Based on the above investigation, the schematic diagram of the water droplets tailored as wax crystals carriers is depicted in Figure 9. The basic structural units in each wax deposit are exhibited. The evolution of these units elucidated that the distribution change of wax crystals from the continuous oil phase to the oil−water interface mitigates the macro wax deposition of the emulsion.

4. CONCLUSIONS

In this work, wax deposition mitigation of a water-in-waxy oil emulsion was systematically investigated through tailoring water droplets as wax crystal carriers. The interfacial action of wax crystals was discerned as adsorption by Span 80 and crystallization by Span 60 through the thermal test and microscopy observation. The wax interfacial crystallization facilitated by Span 60 significantly altered the original solidification site of wax from the continuous oil phase to the oil−water interface, which was regarded as the decisive change to achieve the wax deposition mitigation effect.

When the Span 60-doped emulsion was used to conduct the wax deposition experiment, tiny nascent wax crystals were first formed at the oil−water interface and naturally integrated with water droplets. Under the stirring condition of the cold finger setup, water droplets entrained wax crystals to disperse in emulsion, reducing the amount of wax crystals available to form the deposit network. In addition, the morphology of the wax deposit from the three emulsions displayed the evolution of the deposit structures, which was also used to verify the mitigation effect. Three basic structural units: (1) water droplet flocs; (2) wax crystal clusters; and (3) wax crystal−water droplet agglomerations were detected in the deposit of the 0.5 wt % Span 80-doped emulsion. However, with the increase of Span 60 used in the emulsion, the wax crystal clusters- and/or networks-dominated deposit was gradually converted into the water droplet flocs-occupied deposit.

Such findings may expand the potential application of interfacial actions to multiphase flow of petroleum, which can be used to resolve the deposition or gelation problems of solidified particles in petroleum under flowing conditions.

■ ASSOCIATED CONTENT

Supporting Information

The Supporting Information is available free of charge at https://pubs.acs.org/doi/10.1021/acsomega.2c06809.

The distribution position of wax crystals for three emulsions with a statistically significant difference (PDF)

■ AUTHOR INFORMATION

Corresponding Author

Qianli Ma − *Jiangsu Key Laboratory of Oil and Gas Storage and Transportation Technology, Changzhou University, Changzhou, Jiangsu 213164, China;* orcid.org/0000-0002-2679-617X; Email: qianlima@cczu.edu.cn

Authors

Chuanshuo Wang − *Jiangsu Key Laboratory of Oil and Gas Storage and Transportation Technology, Changzhou University, Changzhou, Jiangsu 213164, China*

Yingda Lu − *Hildebrand Department of Petroleum & Geosystems Engineering, The University of Texas at Austin, Austin, Texas 78712, United States;* orcid.org/0000-0002-7469-117X

Yang Liu − *Jiangsu Key Laboratory of Oil and Gas Storage and Transportation Technology, Changzhou University, Changzhou, Jiangsu 213164, China*

Xiaofang Lv − *Jiangsu Key Laboratory of Oil and Gas Storage and Transportation Technology, Changzhou University, Changzhou, Jiangsu 213164, China; Institute of Petroleum Engineering Technology, Sinopec Northwest Oil Field Company, Urumqi, Xinjiang 830011, China*

Shidong Zhou − *Jiangsu Key Laboratory of Oil and Gas Storage and Transportation Technology, Changzhou University, Changzhou, Jiangsu 213164, China;* orcid.org/0000-0001-8468-1226

https://doi.org/10.1021/acsomega.2c06809
ACS Omega 2023, 8, 7546−7554

Jing Gong − *National Engineering Laboratory for Pipeline Safety, MOE Key Laboratory of Petroleum Engineering, and Beijing Key Laboratory of Urban Oil and Gas Distribution Technology, China University of Petroleum-Beijing, Beijing 102249, China*

Complete contact information is available at: https://pubs.acs.org/10.1021/acsomega.2c06809

Author Contributions

Q.M.: conceptualization, methodology, writing—original draft, and investigation. Y.L.: investigation and data curation. Y.L.: writing—review and editing. X.L.: formal analysis. S.Z.: resources. C.W.: validation. J.G.: project administration.

Notes

The authors declare no competing financial interest.

■ ACKNOWLEDGMENTS

This work was supported by the National Natural Science Foundation of China [nos. 52004039 and 52274061], the China Postdoctoral Science Foundation [no. 2021M693908], and the funds for 2021 scientific research in Changzhou University [no. ZMF21020381], which are gratefully acknowledged.

■ REFERENCES

(1) Rousseau, D. Aqueous droplets as active fillers in oil-continuous emulsions. *Curr. Opin. Food Sci.* **2020**, *33*, 173−186.
(2) Rafanan, R.; Rousseau, D. Dispersed droplets as tunable fillers in water-in-oil emulsions stabilized with fat crystals. *J. Food Eng.* **2019**, *244*, 192−201.
(3) Rafanan, R.; Rousseau, D. Dispersed droplets as active fillers in fat-crystal network-stabilized water-in-oil emulsions. *Food Res. Int.* **2017**, *99*, 355−362.
(4) Wijarnprecha, K.; de Vries, A.; Santiwattana, P.; Sonwai, S.; Rousseau, D. Rheology and structure of oleogelled water-in-oil emulsions containing dispersed aqueous droplets as inactive fillers. *LWT−Food Sci. Technol.* **2019**, *115*, 108067.
(5) Di Bari, V.; Macnaughtan, W.; Norton, J.; Sullo, A.; Nortonb, I. Crystallisation in water-in-cocoa butter emulsions: Role of the dispersed phase on fat crystallisation and polymorphic transition. *Food Struct.* **2017**, *12*, 82−93.
(6) Le Révérend, B. J. D.; Taylor, M. S.; Norton, I. T. Design and application of water-in-oil emulsions for use in lipstick formulations. *Int. J. Cosmet. Sci.* **2011**, *33*, 263−268.
(7) Ghosh, S.; Pradhan, M.; Patel, T.; Haj-shafiei, S.; Rousseau, D. Long-term stability of crystal-stabilized water-in-oil emulsions. *J. Colloid Interface Sci.* **2015**, *460*, 247−257.
(8) Ghosh, S.; Rousseau, D. Triacylglycerol Interfacial Crystallization and Shear Structuring in Water-in-Oil Emulsions. *Cryst. Growth Des.* **2012**, *12*, 4944−4954.
(9) Hodge, S. M.; Rousseau, D. Continuous-Phase Fat Crystals Strongly Influence Water-in-Oil Emulsion Stability. *J. Am. Oil Chem. Soc.* **2005**, *82*, 159−164.
(10) Rousseau, D.; Hodge, S. M. Stabilization of water-in-oil emulsions with continuous phase crystals. *Colloids Surf., A* **2005**, *260*, 229−237.
(11) Ma, Q.; Wang, W.; Liu, Y.; Yang, J.; Shi, B.; Gong, J. Wax adsorption at paraffin oil-water interface stabilized by Span80. *Colloids Surf., A* **2017**, *518*, 73−79.
(12) Chen, X.; Li, C.; Liu, D.; Li, B.; Zhang, H.; Yang, F.; Sun, G.; Dai, S.; Zhao, Y. Effect of doped emulsifiers on the morphology of precipitated wax crystals and the gel structure of water-in-model-oil emulsions. *Colloids Surf., A* **2020**, *607*, 125434.
(13) Li, Y.; Li, C.; Sun, G.; Chen, X.; Liu, D.; Yang, F.; Yao, B.; Zhao, Y. Characterization of the Precipitation Modes of Paraffin Wax in Water-in-Model-Oil Emulsions. *Energy Fuels* **2020**, *34*, 16014−16022.
(14) Szumała, P.; Luty, N. Effect of different crystalline structures on W/O and O/W/O waxemulsion stability. *Colloids Surf., A* **2016**, *499*, 131−140.
(15) Haj-shafiei, S.; Ghosh, S.; Rousseau, D. Kinetic stability and rheology of wax-stabilized water-in-oil emulsions at different water cuts. *J. Colloid Interface Sci.* **2013**, *410*, 11−20.
(16) Ghosh, S.; Tran, T.; Rousseau, D. Comparison of Pickering and Network Stabilization in Water-in-Oil Emulsions. *Langmuir* **2011**, *27*, 6589−6597.
(17) Wassell, P.; Okamura, A.; Young, N. W. G.; Bonwick, G.; Smith, C.; Sato, K.; Ueno, S. Synchrotron Radiation Macrobeam and Microbeam X-ray Diffraction Studies of Interfacial Crystallization of Fats in Water-in-Oil Emulsions. *Langmuir* **2012**, *28*, 5539−5547.
(18) Shinohara, Y.; Takamizawa, T.; Ueno, S.; Sato, K. Microbeam X-ray Diffraction Analysis of Interfacial Heterogeneous Nucleation of n-Hexadecane inside Oil-in-Water Emulsion Droplets. *Cryst. Growth Des.* **2008**, *8*, 3123−3126.
(19) Ueno, S.; Hamada, Y.; Sato, K. Controlling Polymorphic Crystallization of n-Alkane Crystals in Emulsion Droplets through Interfacial Heterogeneous Nucleation. *Cryst. Growth Des.* **2003**, *3*, 935−939.
(20) Kaneko, N.; Horie, T.; Ueno, S.; Yano, J.; Katsuragi, T.; Sato, K. Impurity effects on crystallization rates of n-hexadecane in oil-in-water emulsions. *J. Cryst. Growth* **1999**, *197*, 263−270.
(21) Sun, G.; Li, C.; Yang, F.; Yao, B.; Xiao, Z. Experimental Investigation on the Gelation Process and Gel Structure of Water-in-Waxy Crude Oil Emulsion. *Energy Fuels* **2017**, *31*, 271−278.
(22) Piroozian, A.; Hemmati, M.; Ismail, I.; Manan, M. A.; Bayat, A. E.; Mohsin, R. Effect of emulsified water on the wax appearance temperature of water-in-waxy-crude-oil emulsions. *Thermochim. Acta* **2016**, *637*, 132−142.
(23) Binks, B. P. Particles as surfactants-similarities and differences. *Curr. Opin. Colloid Interface Sci.* **2002**, *7*, 21−41.
(24) Chevalier, Y.; Bolzinger, M. A. Emulsions stabilized with solid nanoparticles: Pickering emulsions. *Colloids Surf., A* **2013**, *439*, 23−34.
(25) Hodge, S. M.; Rousseau, D. Flocculation and coalescence in water-in-oil emulsions stabilized by paraffin wax crystals. *Food Res. Int.* **2003**, *36*, 695−702.
(26) Zhou, X.; Wang, Y.; Zhang, L.; Zhang, K.; Jiang, Q.; Pu, H.; Wang, L.; Yuan, Q. Evaluation of enhanced oil recovery potential using gas/water flooding in a tight oil reservoir. *Fuel* **2020**, *272*, 117706.
(27) Ma, Q.; Wang, W.; Wang, C.; Gong, J. Experimental Investigation of Entrapped Water Droplets in Wax Deposition from Water-in-Oil Emulsion Considering Wax Crystals Adsorption at the Oil-Water Interface. *Energy Fuels* **2020**, *34*, 1601−1607.
(28) Singh, P.; Venkatesan, R.; Fogler, H. S.; Nagarajan, N. Formation and Aging of Incipient Thin Film Wax-Oil Gels. *AIChE J.* **2000**, *46*, 1059−1074.
(29) Wang, Z.; Bai, Y.; Zhang, H.; Liu, Y. Investigation on gelation nucleation kinetics of waxy crude oil emulsions by their thermal behavior. *J. Pet. Sci. Eng.* **2019**, *181*, 106230.
(30) Bell, E.; Lu, Y.; Daraboina, N.; Sarica, C. Experimental Investigation of active heating in removal of wax deposits. *J. Pet. Sci. Eng.* **2021**, *200*, 108346.
(31) Gao, X.; Huang, Q.; Zhang, X.; Zhang, Y.; Zhu, X.; Shan, J. Experimental study on the wax removal physics of foam pig in crude oil pipeline pigging. *J. Pet. Sci. Eng.* **2021**, *205*, 108881.
(32) Chi, Y.; Yang, J.; Sarica, C.; Daraboina, N. A Critical Review of Controlling Paraffin Deposition in Production Lines Using Chemicals. *Energy Fuels* **2019**, *33*, 2797−2809.
(33) Katsuragi, T.; Kaneko, N.; Sato, K. Effects of addition of hydrophobic sucrose fatty acid oligoesters on crystallization rates of n-hexadecane in oil-in-water emulsions. *Colloids Surf., B* **2001**, *20*, 229−237.

(34) Wang, W.; Huang, Q.; Zheng, H.; Li, S.; Long, Z.; Wang, Q. Investigation of wax deposition and effective diffusion coefficient in water-in-oil emulsion system. *J. Therm. Anal. Calorim.* **2018**, *134*, 1031−1043.
(35) Li, R.; Huang, Q.; Huo, F.; Fan, K.; Li, W.; Zhang, D. Effect of shear on the thickness of wax deposit under laminar flow regime. *J. Pet. Sci. Eng.* **2019**, *181*, 106212.
(36) Zheng, S.; Fogler, H. S. Fundamental Investigation of Wax Diffusion Characteristics in Water-in-Oil Emulsion. *Ind. Eng. Chem. Res.* **2015**, *54*, 4420−4428.
(37) Zheng, S.; Khrutphisit, T.; Fogler, H. S. Entrapment of Water Droplets in Wax Deposits from Water-in-Oil Dispersion and Its Impact on Deposit Build-up. *Energy Fuels* **2017**, *31*, 340−350.
(38) Ma, Q.; Liu, Y.; Lv, X.; Zhou, S.; Lu, Y.; Wang, C.; Gong, J. In situ record of the dynamic process of wax deposition in water-in-oil emulsion: Evolution of two types of deposition structures. *J. Pet. Sci. Eng.* **2022**, *214*, 110560.

https://doi.org/10.1021/acsomega.2c06809
ACS Omega 2023, 8, 7546−7554